Excitation Performance and SAR Control with Z-Stacked Body RF Coil Arrays in Parallel Transmission at 3T

Xiaotong Zhang[1], Xiaoping Wu[2], Jinfeng Tian[2], Sebastian Schmitter[2], Lance DelaBarre[2], Michael Hamm[3], Josef Pfeuffer[3], Dingxin Wang[2,4], Bin He[1,5], Thomas Vaughan[2], Kamil Ugurbil[2], and Pierre-Francois Van de Moortele[2]

[1]Department of Biomedical Engineering, University of Minnesota, Minneapolis, MN, United States, [2]Center for Magnetic Resonance Research, University of Minnesota, Minneapolis, MN, United States, [3]3Siemens Healthcare, MR Application Development, Erlangen, Germany, [4]Siemens Medical Solutions USA Inc, Minneapolis, MN, United States, [5]Institute for Engineering in Medicine, University of Minnesota, Minneapolis, MN, United States

Audience: RF Coil engineers, MR Physicists, Electromagnetic Model builders, RF pulse designers, Radiologists.

Purpose: In z-stacked transmit coil arrays[1-3], coil elements are distributed along z-axis to enable B1 manipulations along *z*. This concept was initially demonstrated to improve excitation homogeneity in the brain[1-5] at 7T. However, transmit B1 (B_1^+) inhomogeneity also affects 3T, especially to image the body the size of which is within RF wavelength range; 3T transmit arrays[2,3,6-10], including z-stacked loop[11] or TEM[8,10] design, can improve excitation patterns and reduce SAR with parallel transmit (pTX) strategies with superior results for z-stacked coils[8,10,11]. Here we focus on TEM arrays, after previous work[8] demonstrating in the pelvis at 3T higher performance of two 8-TEM arrays stacked along z, compared with a single array. We expand this investigation to 3 different 3T TEM arrays (chosen from a pool of modeled coils[10]) including two z-stacked structures, and to spine and brain targets; we compare excitation fidelity, RF power (pwr), global SAR and peak 10-gram average local SAR (10gSAR). RF Spoke placement impact is further detailed for different coil designs.

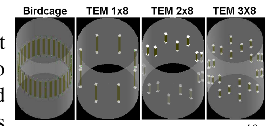

Fig.1. Body coil structures[10].

Methods: Three TEM whole body arrays consisting of one ring (1x8), 2 z-stacked rings (2x8) or 3 z-stacked rings (3x8) of TEM elements (8 per ring) were modeled in XFtdt (Remcom, PA), as well as a High Pass birdcage (32 rungs) driven on two quad ports (1x2) and used as conventional reference (Fig1). Each coil was loaded with the Duke body model (from Virtual Family[3,12], 5mm isotropic). For each target, the volume of interest (VOI) was co-centered along *z* with the RF coil. Single and 2-spoke pTx pulses were designed aiming at a uniform 10° excitation flip angle (FA) in tissues included in a box-shaped VOI covering, along *x*- & *z*-axes: 32cm×39cm (pelvis), 8cm×40cm (spine, white VOI Fig.3) and 20cm×39cm (brain+c-spine). All tissues were included along *y*-axis; voxels outside VOI were ignored. A magnitude least square problem[13] was designed: $\min_\omega \| |A\omega| - 1 \|_2^2 + \lambda R(\omega)$, with $R(\omega)$ as either total RF pwr: $\|\omega\|_2^2$, global SAR: $\|S_0\omega\|_2^2$, or peak 10g SAR: $\Sigma_n \alpha_n \|S_n\omega\|_2^2$; S_0 the global SAR matrix, $n \in [1, N_{VOP}]$ where N_{VOP} is the number of virtual observation points[14] (VOP), S_n is the *n*-derived SAR matrix and α_n weighs the *n*-th VOP peak SAR. For 2-spoke pulses, symmetric 3D k-space polar coordinates (radius, ±[φ,θ]) were optimized through exhaustive search (23 radii from 0 to 10 m^{-1}, 15° phase steps [0-180°] for φ and θ, i.e. 3312 trials for each λ) to minimize total RF pwr or global SAR. The best spoke location to minimize global SAR for a given RMSE was used to minimize local peak SAR at the same RMSE level.

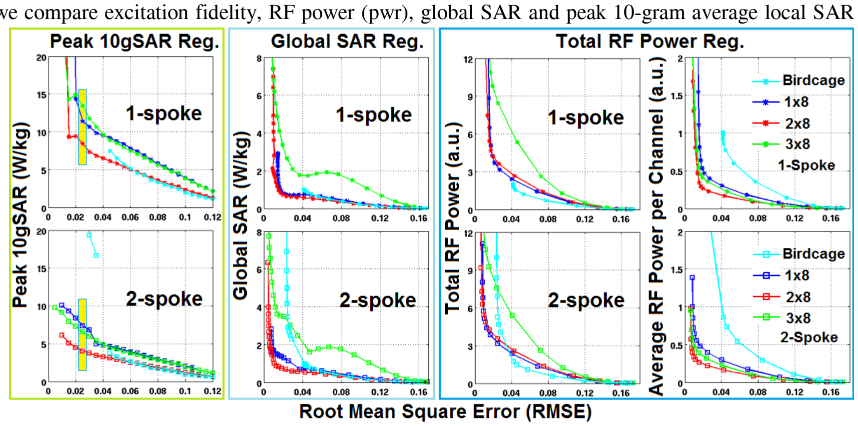

Fig2 Regularization criteria. 'Reg.' in top title. Each point on a curve for a different λ.

Results: **Target=spine.** L-curves (Fig.2) show root mean square error (RMSE) of resulting FA vs. uniform 10° for Single (upper row) and 2-Spoke (lower row) pulses. Main findings: smaller RMSE could always be achieved by any TEM array than the Birdcage coil. 2x8-TEM consistently outperforms all other coils for SAR constraints, an advantage most pronounced for *peak 10gSAR* constraint. For *global* SAR, and even more so for RF Pwr constraint, 1x8 and 2x8 TEM are closer to each other. Overall 3x8-TEM is poorly efficient, matching at best 1x8 TEM in some configurations. 2-spoke pulses outperform single-spoke for all metrics and coils, with the strongest gain for peak 10gSAR control. Fig.3 shows peak 10gSAR constraint results: peak 10gSAR Maximum Intensity Projection (MIP) for fixed RMSE=0.025 (yellow box in Fig.2) shows dramatic reduction with i) 2x8-TEM and ii) 2-spoke pulses. Birdcage results are not shown because RMSE=0.025 either can't be reached or require a large SAR beyond the plotted range. Other metrics: coefficient of variation (CV=std/mean) of FA and min/max/avg RF pwr per channel. Similar results were also observed in brain and pelvis targets. A crucial role of spoke 3D k-space location is demonstrated in Fig.4 (target: spine, with global SAR constraint for 2x8 TEM) where exhaustive search for each λ yields large (single colored) stretches (retained values shown in light green curves); note the remarkable pattern consistency through coils.

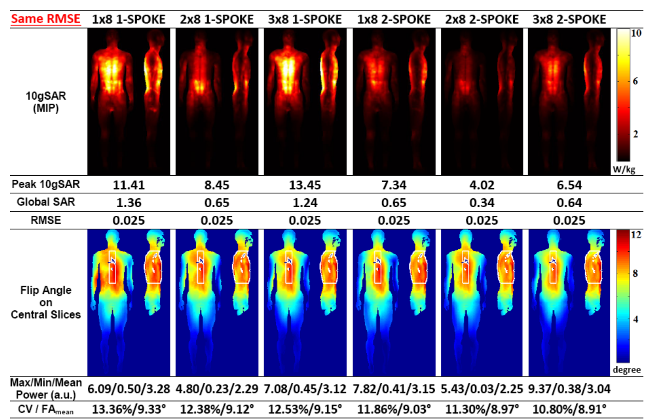

Fig.3. VOI: spine. Performance comparison of body arrays with peak 10gSAR constraint at fixed RMSE=0.025.

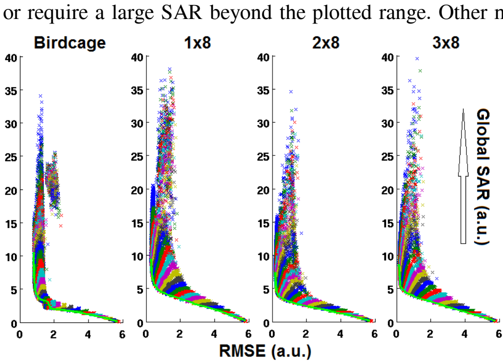

Fig.4. RMSE against Global SAR. All 3D k-space spoke placements for a given λ value in a same color.

Discussion: All TEM arrays can achieve significantly higher excitation fidelity than the Birdcage coil, even though the latter is driven as a 2-ch pTX coil. The best performing coil (2x8 TEM) is a z-stacked array and excels the most at reducing peak 10gSAR, which is arguably one of the most significant criteria to address scanner limitations due to patient safety. There is a cost in required RF pwr when using TEM arrays; although total RF pwr increase was limited (not shown) with 1x8 or 2x8 TEM, the per-channel max RF pwr substantially increased, pointing towards the need for additional constraints to limit max RF pwr per channel in RF pulse design[15].

Refs: 1) Adriany, ISMRM'07, 166. 2) Vaughan, John Wiley & Sons'11. 3) Vaughan, John Wiley & Sons'12. 4) Ritter, ISMRM'11, 3590. 5) Wu, ISMRM'12, 638. 6) Vernickel, MRM 58:381. 7) Ryu, ISMRM'12, 2613. 8) Wu, ISMRM'13, 4398. 9) Guerin, ISMRM'12, 2215. 10) Tian, ISMRM'13, 2746. 11) Guerin, ISMRM'13, 2741. 12) Christ, PMB 55:1767. 13) Setsompop, MRM 60:1422. 14) Eichfelder, MRM 66:1468. 15) Guerin, MRM doi:10.1001/mrm24800.

Grant support: NIH EB015894, EB006385 EB017069-01A1, Siemens research grant.